$K\bar{K}N$ molecule state with $I = 1/2$ and $J^P = 1/2^+$ studied with a three-body calculation

Daisuke Jido and Yoshiko Kanada-En'yo
Yukawa Institute for Theoretical Physics, Kyoto University, Kyoto 606-8502, Japan
(Received 22 June 2008; published 16 September 2008)

A $K\bar{K}N$ system with $I = 1/2$ and $J^P = 1/2^+$ is investigated with nonrelativistic three-body calculations by using effective $\bar{K}N$, $K\bar{K}$, and KN interactions. The $\bar{K}N$ interaction describes the $\Lambda(1405)$ as a $\bar{K}N$ molecule, and the $K\bar{K}$ interaction is adjusted to give $f_0(980)$ and $a_0(980)$ states as $K\bar{K}$ molecules. The present investigation suggests that a bound $K\bar{K}N$ state can be formed below the $K\bar{K}N$ threshold (1930 MeV) with a $90 \sim 100$ MeV width of three-hadron decays, which are dominated by $K\bar{K}N \to K\pi\Sigma$ and $\pi\eta N$. The $K\bar{K}N$ state is found to be a weakly bound hadron molecular state with a size larger than an α particle because of the repulsive KN interactions.

DOI: 10.1103/PhysRevC.78.035203 PACS number(s): 14.20.Gk, 13.75.Jz, 13.30.Eg, 21.45.−v

I. INTRODUCTION

Exploring composite systems of mesons and baryons is a challenging issue both in theoretical and experimental hadron-nuclear physics. One of the historical examples in two-hadron systems is $\Lambda(1405)$ as a quasibound state of $\bar{K}N$ [1]. For mesonic resonances, the scalar mesons, $f_0(980)$ and $a_0(980)$, are also the candidates of the hadronic molecular states [2]. Baryon resonances as three-hadron systems have been also investigated theoretically for systems of πKN [3–5], $\pi\bar{K}N$ [6], and $\bar{K}\bar{K}N$ [7,8]. Based on the idea to regard $\Lambda(1405)$ as a $\bar{K}N$ quasibound state [9,10], bound systems of a few nucleons with antikaon were investigated in Refs. [9–16].

Recently a baryonic resonance with $J^P = 1/2^+$ and $S = -2$ composed by $\bar{K}\bar{K}N$ has been studied in details by the authors in Ref. [8] based on three-body calculation with attractive $\bar{K}N$ interactions given by Refs. [9,15,17]. In this system, the antikaons play unique roles, because they have enough attraction with the nucleon to form a quasibound state as $\Lambda(1405)$ and possess so heavy mass to provide small kinetic energy in the $\bar{K}\bar{K}N$ system. The quasibound state of $\bar{K}\bar{K}N$ has a characteristic structure that one of the antikaons forms $\Lambda(1405)$ with the nucleon [$\Lambda(1405)$ cluster] as seen also in K^-pp system [12], and the other antikaon spreads for long distance. This structure is caused by strong $\bar{K}N$ attraction with $I = 0$.

In this article, we explore quasibound states of the $K\bar{K}N$ system with $I = 1/2$ and $J^P = 1/2^+$, assuming that the $\bar{K}N$ and $K\bar{K}$ systems have enough attractions to form quasibound states of $\Lambda(1405)$ in $I = 0$ and $f_0(980)$ [$a_0(980)$] in $I = 0$ ($I = 1$), respectively. We use the effective interactions of $\bar{K}N$ extracted by Akaishi-Yamazaki (AY) [9,15] and Hyodo-Weise (HW) [17] in phenomenological way and chiral dynamics, respectively. These interaction provide $\Lambda(1405)$ as a quasibound state with $I = 0$ and also weak attraction in the $I = 1$ channel. The effective $K\bar{K}$ interactions are adjusted to reproduce the masses and the widths of $f_0(980)$ and $a_0(980)$ as the $K\bar{K}$ molecular states. The KN interactions are known to have strong repulsion in $I = 1$ channel. We use the KN potential fitted by deduced scattering lengths.

The "fate" of the $K\bar{K}N$ molecular state strongly depends on its binding energy. If the energy of the $K\bar{K}N$ system is above the lowest threshold of the subcomponents, the $K\bar{K}N$ states can decay to the subcomponents and the width gets very large. If the $K\bar{K}N$ state is bound with moderate binding energy below all the thresholds of $\Lambda(1405) + K$, $f_0(980) + N$, and $a_0(980) + N$, the state is quasistable against these decay modes and has comparable decay width with those of the two-particle subsystems. For more deeply bound $K\bar{K}N$ system, because the constituents largely overlap each other, the molecular picture may be broken down and two-body decays are enhanced.

Having strong attractions in $\bar{K}N$ and $K\bar{K}$ subsystems, it is naturally expected that $K\bar{K}N$ forms a hadron molecule below the thresholds of $\Lambda(1405) + K$ and $f_0(a_0) + N$. The question arising here is whether the attractions are so strong that the hadronic molecular picture breaks down in deeply bound state and the quasibound state has large width, or in opposite direction, whether or not the repulsion of KN is too strong for spoiling the bound state.

In Sec. II, we describe the framework of the present calculations. We apply a variational approach with a Gaussian expansion method [18] to solve the Schrödinger equation of the three-body system. By treating the imaginary potentials perturbatively, we find the $K\bar{K}N$ quasibound state. In Sec. III, we present our results of the three-body calculation. In analysis of the wave functions, we discuss the structure of the $K\bar{K}N$ state. Section IV is devoted to summary of this work.

II. FORMULATION

We apply a nonrelativistic three-body potential model for the $K\bar{K}N$ system. The effective two-body interactions are given in local potential forms. The $K\bar{K}N$ wave function is calculated by solving Schrödinger equation with a Gaussian expansion method for the three-body system. In this section, we briefly explain the formulation and interactions used in the present work. The details of the formulation and the $\bar{K}N$ interaction are discussed in Ref. [8].

A. Hamiltonian

In the present work, the Hamiltonian for the $K\bar{K}N$ system is given by

$$H = T + V \tag{1}$$

$$V \equiv V_{\bar{K}N}(r_1) + V_{KN}(r_2) + V_{K\bar{K}}(r_3), \tag{2}$$

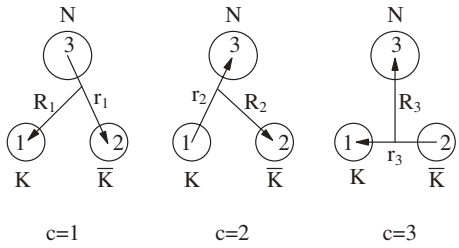

FIG. 1. Three Jacobian coordinates of the $K\bar{K}N$ system.

with the kinetic energy T and the potential energy V, which consists of the effective $\bar{K}N$ interaction $V_{\bar{K}N}$, the KN interaction V_{KN}, and the $K\bar{K}$ interaction $V_{K\bar{K}}$. These interactions are given by ℓ-independent local potentials as functions of $\bar{K}$-N, K-N, and K-$\bar{K}$ distances, r_1, r_2, and r_3 defined by $r_1 = |\mathbf{x}_{\bar{K}} - \mathbf{x}_N|$, $r_2 = |\mathbf{x}_N - \mathbf{x}_K|$, and $r_3 = |\mathbf{x}_K - \mathbf{x}_{\bar{K}}|$, respectively, with spatial coordinates $\mathbf{x}_K$, $\mathbf{x}_{\bar{K}}$, $\mathbf{x}_N$ for the kaon, the antikaon, and the nucleon. For convenience, we introduce Jacobian coordinates, $\mathbf{r}_c$ and $\mathbf{R}_c$, in three rearrangement channels $c = 1, 2, 3$ as shown in Fig. 1. We assume isospin symmetry in the effective interactions, and we also neglect the mass difference among $K^{\pm}$, $\bar{K}^0$, and K^0, and that between proton and neutron by using the averaged masses, $M_K = 495.7$ MeV and $M_N = 938.9$ MeV. We do not consider three-body forces nor transitions to two-hadron decays, which will be important if the constituent hadrons are localized in a small region.

The kinetic energy T is simply given by the Jacobian coordinates with one of the rearrangement channels as

$$T \equiv \frac{-1}{2\mu_{r_c}}\nabla^2_{r_c} + \frac{-1}{2\mu_{R_c}}\nabla^2_{R_c}, \tag{3}$$

with the reduced masses μ_{r_c} and μ_{R_c} for the corresponding configuration, for instance, $\mu_{r_1} = M_K M_N/(M_K + M_N)$ and $\mu_{R_1} = M_K(M_K + M_N)/(2M_K + M_N)$ for the rearrangement channel $c = 1$.

The effective interactions, $V_{\bar{K}N}$, V_{KN}, and $V_{K\bar{K}}$, are obtained by s-wave two-body scattering with isospin symmetry. The explicit expression of the effective interactions will be given in Sec. II B. Open channels of $\bar{K}N$ and $K\bar{K}$ ($\pi\Lambda$ and $\pi\Sigma$ for $\bar{K}N$, $\pi\pi$ and $\pi\eta$ for $K\bar{K}$) are implemented effectively to the imaginary parts of the interactions $V_{\bar{K}N}$ and $V_{K\bar{K}}$. Consequently, the Hamiltonian (1) is not Hermitian. In solving Schrödinger equation for $K\bar{K}N$, we first take only the real part of the potentials and obtain wave functions in a variational approach. Then we calculate bound-state energies E as expectation values of the total Hamiltonian (1) with respect to the obtained wave functions. The widths of the bound states are evaluated by the imaginary part of the complex energies as $\Gamma = -2\mathrm{Im}E$.

B. Effective interactions

In this subsection, we explain the details of the effective interactions of the $\bar{K}N$, $K\bar{K}$, and KN two-body subsystems in our formulation. The interaction parameters and the properties of the two-body subsystems are listed in Table I.

TABLE I. The interaction parameters and the properties of two-body systems. The energies (E) are evaluated from the corresponding two-body threshold. They are calculated by treating the imaginary part of the two-body potentials perturbatively. We also list the root-mean-square two-body distances of the $\bar{K}N(I = 0)$, $K\bar{K}(I = 0)$ and $K\bar{K}(I = 1)$ states, which correspond to $\Lambda(1405)$ and $f_0(980)$, $a_0(980)$, respectively. For the $K\bar{K}$ interactions, we show the scattering lengths obtained in the present parameters.

	Parameter set of interactions (A)	(B)
$\bar{K}N$	HW-HNJH	AY
b (fm)	0.47	0.66
$U^{I=0}_{\bar{K}N}$ (MeV)	$-908 - 181i$	$-595 - 83i$
$U^{I=1}_{\bar{K}N}$ (MeV)	$-415 - 170i$	$-175 - 105i$
$\bar{K}N(I = 0)$ state		
ReE (MeV)	-11	-31
ImE (MeV)	-22	-20
$\bar{K}$-N distance (fm)	1.9	1.4
$K\bar{K}$	KK(A)	KK(B)
b (fm)	0.47	0.66
$U^{I=0,1}_{K\bar{K}}$ (MeV)	$-1155 - 283i$	$-630 - 210i$
$K\bar{K}(I = 0, 1)$ state		
ReE (MeV)	-11	-11
ImE (MeV)	-30	-30
K-$\bar{K}$ distance (fm)	2.1	2.2
KN	KN(A)	KN(B)
b (fm)	0.47	0.66
$U^{I=0}_{KN}$ (MeV)	0	0
$U^{I=1}_{KN}$ (MeV)	820	231
$a^{I=0}_{KN}$ (fm)	0	0
$a^{I=1}_{KN}$ (fm)	-0.31	-0.31

1. $\bar{K}N$ interaction

In this work, we use the same $\bar{K}N$ potential as used in Ref. [8] for the $\bar{K}\bar{K}N$ calculations. We consider two different effective $\bar{K}N$ interactions to estimate theoretical uncertainties. These two interactions were derived in different ways. One of the $\bar{K}N$ interaction that we use is given by Hyodo and Weise in Ref. [17] and was derived based on the chiral unitary approach for s-wave scattering amplitude with strangeness $S = -1$. The other interaction is Akaishi-Yamazaki (AY) potential derived phenomenologically by using $\bar{K}N$ scattering and kaonic hydrogen data and reproducing the $\Lambda(1405)$ resonance as a $K^- p$ bound state at 1405 MeV [9,15]. Both $\bar{K}N$ interactions have so strong attraction in $I = 0$ as to provide the $\Lambda(1405)$ as a quasibound state of the $\bar{K}N$ system, and have weak attraction in $I = 1$. Hereafter we refer the quasibound $\bar{K}N$ state as $\{\bar{K}N\}_{I=0}$.

The potential is written in a one-range Gaussian form as

$$V_{\bar{K}N} = U^{I=0}_{\bar{K}N}\exp[-(r/b)^2]P_{\bar{K}N}(I = 0) + U^{I=1}_{\bar{K}N}\exp[-(r/b)^2]P_{\bar{K}N}(I = 1), \tag{4}$$

with the isospin projection operator $P_{\bar{K}N}(I = 0, 1)$ and the range parameter b. The potential depth $U^I_{\bar{K}N}$ are given in a complex number reflecting the effects of the open channel of $\pi\Sigma$ and $\pi\Lambda$. The numbers for b and $U^I_{\bar{K}N}$ are given in Table I. For the Hyodo-Weise potential, we use the parameter set referred as HNJH in Ref. [17], which was obtained by the chiral unitary model with the parameters of Ref. [19]. We refer this potential as the HW-HNJH potential. The energy of the HW-HNJH potential is fixed at $\omega = M_K + M_N - 11$ MeV, which is the resonance position of $\Lambda(1405)$, because the energy dependence in the potential is small in the region of $\omega =$ 1400 MeV to the $\bar{K}N$ threshold, and it was found in Ref. [8] that the results for the $\bar{K}\bar{K}N$ system were not sensitive to the choice of the energy. In the present system, we have also calculated the bound state energy with the $\bar{K}N$ potential for the $\bar{K}N$ energy at the threshold $\omega = M_K + M_N$ and confirmed that the energy (ω) dependence of the HW-HNJH potential is small in the result.

The important difference between the two interactions of AY and HW-HNJH is the binding energy of the $\bar{K}N$ system. In chiral unitary approaches for the meson-baryon interactions, the $\Lambda(1405)$ resonance is described as a $\bar{K}N$ quasibound state [20] located at $\omega \sim 1420$ MeV in $\bar{K}N$ scattering amplitude [21]. This is a consequence of the double pole nature that $\Lambda(1405)$ is described by superposition of two poles as found in Refs. [21–23]. For the AY potential, the $\Lambda(1405)$ resonance was reproduced at $\sim$1405 MeV as the Particle Date Group (PDG) reported. Thus, the AY potential has stronger attraction in $I = 0$ than the HW-HNJH potential. The properties of the $\bar{K}N$ two-body system obtained by these potentials are summarized in Table I.

It is interesting pointing out that the real energy calculated in the perturbative treatment with the HW-HNJH agrees with the resonance position of the $\bar{K}N \to \bar{K}N$ scattering amplitude with $I = 0$ shown in Ref. [17]. There with the energy-dependent local effective potential, which is used in the present work with energy fixing, they have calculated the $\bar{K}N \to \bar{K}N$ scattering amplitude with $I = 0$. For this scattering amplitude, the resonance position, where the real part of the amplitude crosses zero and the imaginary part is maximum, can be read as around 1425 MeV, which corresponds to -9 MeV measured from the threshold.

2. $K\bar{K}$ interaction

The $K\bar{K}$ interaction is derived in the present work under the assumption that $K\bar{K}$ forms quasibound states in $I = 0$ and $I = 1$, which correspond to $f_0(980)$ and $a_0(980)$, respectively. Thus, we use strong effective single-channel $K\bar{K}$ interactions that reproduce the masses and widths of $f_0(980)$ and $a_0(980)$ as the quasibound $K\bar{K}$ states. We refer the quasibound $K\bar{K}$ states as $\{K\bar{K}\}_{I=0,1}$.

We take the one-range Gaussian form,

$$V^{I=0,1}_{K\bar{K}}(r) = U^{I=0,1}_{K\bar{K}} \exp[-(r/b)^2] P_{K\bar{K}}(I = 0, 1), \qquad (5)$$

where the range parameter b is chosen to be the same value as that of the $\bar{K}N$ interaction. We adjust the strength $U^{I=0,1}_{K\bar{K}}$ to fit the $f_0(980)$ and $a_0(980)$ masses and the widths with the energies of two-body calculations of the $K\bar{K}$ system. The PDG reports [24] the $f_0(980)$ and $a_0(980)$ have 980 ± 10 MeV and 984.6 ± 1.2 MeV masses with the 40–100 MeV and 50–100 MeV widths, respectively, in average of the compilation of the experimental data. The dominant decay modes are $\pi\pi$ for $f_0(980)$ and $\pi\eta$ for $a_0(980)$. We take the mass 980 MeV and the width 60 MeV as the inputs to determine the $K\bar{K}$ interactions in both the $I = 0$ and $I = 1$ channels. Then we get $U^{I=0,1}_{K\bar{K}} = -1155 - 283i$ MeV for $b =$ 0.47 fm and $U^{I=0,1}_{K\bar{K}} = -630 - 210i$ MeV for $b = 0.66$ fm, by fitting the energies of the $K\bar{K}$ bound states to the meson masses and the widths. We refer to the former potential as KK(A) and the latter as KK(B). In this phenomenological single-channel interaction, the effect of the two-meson decays such as $\pi\pi$ and $\pi\eta$ decays is incorporated in the imaginary part of the effective $K\bar{K}$ interaction.

In the present parametrization of the $K\bar{K}$ potential, we have fitted the potential strengths to reproduce the PDG values of the $f_0(980)$ and $a_0(980)$ masses as bound-state energies of $K\bar{K}$ calculated with the perturbative treatment of the imaginary potential. When we directly calculate the pole position of the $K\bar{K}$ scattering amplitude in Lippmann-Schwinger equation with the present potential, we get the value $998 - 32i$ MeV for the parameter set (A). This is obtained above the $K\bar{K}$ threshold in the first Riemann sheet as a virtual state. Namely the $K\bar{K}$ channel is *closed* and this resonance is *not* one decaying to $K\bar{K}$ even though it locates energetically above the threshold. The pole obtained here is consistent with the pole position of scattering amplitude calculated by the chiral unitary approach [25,26]. In the chiral unitary approach, s-wave scattering amplitudes with $I = 0$ and $I = 1$ were reproduced well by coupled channels of $\pi\pi$, $\pi\eta$, and $K\bar{K}$. The $f_0(980)$ and $a_0(980)$ meson are obtained as the resonance poles at 993.5 MeV for $f_0(980)$ and 1009.2 MeV for $a_0(980)$ [26]. The f_0 is described dominantly by $K\bar{K}$ scattering, whereas for a_0 the $\pi\eta$ scattering is also important as well as $K\bar{K}$ scattering. These values are slightly higher than the masses reported by PDG, which are given by the peak position of the spectra. We will discuss ambiguity of the $K\bar{K}$ interactions in later section.

3. KN interaction

We construct the KN interaction based on deduced KN scattering lengths from the KN phase shifts [27]. The KN interactions are known to be strong repulsion in the $I =$ 1 channel and very weak in the $I = 0$ channel. The experimental values of the scattering lengths for the $I = 0$ and $I = 1$ channels are $a^{I=0}_{KN} = -0.035$ fm and $a^{I=1}_{KN} = -0.310 \pm 0.003$ fm [27]. In the present calculation, we assume no interaction in the $I = 0$ channel. For the $I = 1$ channel, we use phenomenological interaction with the one-range Gaussian form again,

$$V^{I=1}_{KN}(r) = U^{I=1}_{KN} \exp[-(r/b)^2] P_{NK}(I = 1), \qquad (6)$$

where the range parameter b is chosen to be the same value as that of the $\bar{K}N$ interaction. We adjust the strength $U^{I=1}_{KN}$ to reproduce the experimental scattering strength and obtain $U^{I=1}_{KN} = 820$ MeV and $U^{I=1}_{KN} = 231$ MeV for $b =$ 0.47 fm and $b = 0.66$ fm, respectively. We refer to the former parametrization as KN(A) and to the latter one as KN(B).

C. Three-body wave function

The three-body $K\bar{K}N$ wave function Ψ is described as a linear combination of amplitudes $\Phi^{(c)}_{I_{K\bar{K}}}(\mathbf{r}_c, \mathbf{R}_c)$ of three rearrangement channels $c = 1, 2, 3$ (Fig. 1) with a label $I_{K\bar{K}}$ for the total isospins of the $K\bar{K}$ subsystem. In the present calculation, we take the model space limited to $l_c = 0$ and $L_c = 0$ of the orbital-angular momenta for the Jacobian coordinates $\mathbf{r}_c$ and $\mathbf{R}_c$ in the channel c because of the fact that the effective local potentials used in the present calculations are derived in consideration of the s-wave two-body dynamics. Then the wave function of the $K\bar{K}N$ system with $I = 1/2$ and $J^P = 1/2^+$ is written as

$$\Psi = \sum_{c, I_{K\bar{K}}} \Phi^{(c)}_{I_{K\bar{K}}}(\mathbf{r}_c, \mathbf{R}_c)\left[[K\bar{K}]_{I_{K\bar{K}}} N\right]_{I=1/2}, \tag{7}$$

where the $[[K\bar{K}]_{I_{K\bar{K}}} N]_{I=1/2}$ specifies the isospin configuration of the wave function $\Phi^{(c)}_{I_{K\bar{K}}}(\mathbf{r}_c, \mathbf{R}_c)$, meaning that the total isospin $1/2$ for the $K\bar{K}N$ system is given by combination of total isospin $I_{K\bar{K}}$ for the $K\bar{K}$ subsystem and isospin $1/2$ for the nucleon.

The wave function of the $K\bar{K}N$ system is obtained by solving the Schrödinger equation,

$$[T + V_{\bar{K}N}(r_1) + V_{KN}(r_2) + V_{K\bar{K}}(r_3) - E]\Psi = 0. \tag{8}$$

In solving the Schrödinger equation for the $K\bar{K}N$ system, we adopt the Gaussian expansion method for three-body systems given in Ref. [18] as the same way as done in Ref. [8]. The spatial wave function $\Phi^{(c)}_{I_{K\bar{K}}}(\mathbf{r}_c, \mathbf{R}_c)$ of each rearrangement channel and $K\bar{K}$ isospin is written in terms of two Gaussian basis functions, $\phi^G_n(\mathbf{r})$ and $\psi^G_n(\mathbf{R})$, as

$$\Phi^{(c)}_{I_{K\bar{K}}}(\mathbf{r}_c, \mathbf{R}_c) = \sum_{n_c, N_c}^{n_{\max}, N_{\max}} A^{c, I_{K\bar{K}}}_{n_c, N_c} \phi^G_{n_c}(\mathbf{r}_c)\psi^G_{N_c}(\mathbf{R}_c), \tag{9}$$

where $n_{\max}$ and $N_{\max}$ are the numbers of the Gaussian basis and the basis functions are defined by

$$\phi^G_n(\mathbf{r}) = \mathcal{N}_n e^{-\nu_n r^2}, \tag{10}$$

$$\psi^G_n(\mathbf{R}) = \mathcal{N}_N e^{-\lambda_N R^2}, \tag{11}$$

with the normalization constants given by $\mathcal{N}_n = 2(2\nu_n)^{3/4}\pi^{-1/4}$ and $\mathcal{N}_N = 2(2\lambda_N)^{3/4}\pi^{-1/4}$, and the Gaussian ranges, ν_n and λ_N, given by

$$\nu_n = 1/r_n^2, \quad r_n = r_{\min}\left(\frac{r_{\max}}{r_{\min}}\right)^{\frac{n-1}{n_{\max}-1}}, \tag{12}$$

$$\lambda_N = 1/R_N^2, \quad R_N = R_{\min}\left(\frac{R_{\max}}{R_{\min}}\right)^{\frac{N-1}{N_{\max}-1}}. \tag{13}$$

We use the parameters $r_{\min}$, $R_{\min} = 0.2$ fm and $r_{\max}$, $R_{\max} = 20$ fm and $n_{\max}$, $N_{\max} = 15$ for all the channels, $c = 1, 2, 3$. The coefficients $A^{c, I_{K\bar{K}}}_{n_c, N_c}$ are determined by variational principle when we solve the Schrödinger equation.

We treat the imaginary part of the potentials perturbatively. We first calculate the wave function for the real part of the Hamiltonian (H^{Re}) with variational principle in the model space of the Gaussian expansion (9). After this variational calculation, we take the lowest-energy solution. The binding energy $B(K\bar{K}N)$ of the three-body system is given as $B(K\bar{K}N) = -E^{\mathrm{Re}}$.

Next we estimate the imaginary part of the energy for the total Hamiltonian by calculating the expectation value of the imaginary part of the Hamiltonian with the obtained wave function Ψ:

$$E^{\mathrm{Im}} = \langle\Psi|\mathrm{Im}V_{\bar{K}N} + \mathrm{Im}V_{K\bar{K}}|\Psi\rangle. \tag{14}$$

The total energy is given as $E = E^{\mathrm{Re}} + iE^{\mathrm{Im}}$, and the decay width is estimated as $\Gamma = -2E^{\mathrm{Im}}$. In the present calculation, we have only three-body decays such as $\pi\Sigma\bar{K}$, $\pi\Lambda\bar{K}$, $\pi\pi N$, and $\eta\pi N$ decays for the $K\bar{K}N$ state by the model setting.

The perturbative treatment performed above is justified qualitatively in the case of $|\langle\Psi|\mathrm{Im}V|\Psi\rangle| \ll |\langle\Psi|\mathrm{Re}V|\Psi\rangle|$. In the two-body systems, $\bar{K}N$ and $K\bar{K}$, we find that this condition is satisfied reasonably, observing that $|\langle\mathrm{Im}V_{\bar{K}N}\rangle| \sim 20$ MeV is much smaller than $|\langle\mathrm{Re}V_{\bar{K}N}\rangle| \sim 100$ MeV, and $|\langle\mathrm{Im}V_{K\bar{K}}\rangle| \sim 30$ MeV is also smaller than $|\langle\mathrm{Re}V_{K\bar{K}}\rangle| \sim 100$ MeV. Also in the case of the $K\bar{K}N$ system, it is found that the absolute values of the perturbative energy $|\langle\Psi|\mathrm{Im}V|\Psi\rangle| \sim 50$ MeV is much smaller than the real potential energy $|\langle\Psi|\mathrm{Re}V|\Psi\rangle| \sim 200$ MeV in the present calculations. In the Appendix, we discuss the correspondence of the complex energy obtained by the perturbative treatment to that calculated with fully treated imaginary potential in complex energy plane in the case of the two-body systems in more details. There we will see that the imaginary energies obtained in both methods are very similar, whereas the real energies can be slightly pushed up due to higher-order corrections of the perturbative expansion.

We calculate partial energies for two-body subsystems ($\bar{K}N$, $K\bar{K}$, and KN) in the $K\bar{K}N$ state with the two-body Hamiltonians as

$$\begin{aligned}
\mathcal{E}_{\bar{K}N} &\equiv \langle\Psi|T_{\bar{K}N} + V_{\bar{K}N}|\Psi\rangle, \\
\mathcal{E}_{K\bar{K}} &\equiv \langle\Psi|T_{K\bar{K}} + V_{K\bar{K}}|\Psi\rangle, \\
\mathcal{E}_{NK} &\equiv \langle\Psi|T_{KN} + V_{NK}|\Psi\rangle,
\end{aligned} \tag{15}$$

where $T_{\bar{K}N}$, $T_{K\bar{K}}$, and T_{KN} are the kinetic energies for the relative $\bar{K}N$, $K\bar{K}$, and KN motion, respectively, given by

$$T_{\bar{K}N} = \frac{-1}{2\mu_{r_1}}\nabla^2_{r_1}, \tag{16}$$

$$T_{K\bar{K}} = \frac{-1}{2\mu_{r_3}}\nabla^2_{r_3}, \tag{17}$$

$$T_{KN} = \frac{-1}{2\mu_{r_2}}\nabla^2_{r_2}. \tag{18}$$

We note that the sum of the kinetic energies $T_{\bar{K}N} + T_{K\bar{K}} + T_{KN}$ is not equal to the total kinetic energy T. We also calculate the partial energy for the s-wave component of the two-body $\bar{K}N$ subsystem defined by

$$\mathcal{E}^{l_1=0}_{\bar{K}N} \equiv \frac{\langle P(l_1 = 0)\Psi|T_{\bar{K}N} + V_{\bar{K}N}|P(l_1 = 0)\Psi\rangle}{\langle P(l_1 = 0)\Psi|P(l_1 = 0)\Psi\rangle}, \tag{19}$$

where $P(l_1 = 0)$ is the projection operator to $l_1 = 0 \otimes L_1 = 0$ space, whose basis has the orbital-angular momenta $l_1 = 0$ and $L_1 = 0$ for the coordinates $\mathbf{r}_1$ and $\mathbf{R}_1$ in the rearrangement channel $c = 1$. We emphasize that the real part of the partial energy $\mathcal{E}$ is inevitably larger than the lowest energy of the

two-body energy eigenstates. This is because the partial energy is calculated by the expectation value of the two-body Hamiltonian as given in Eq. (15), and the relative two-body wave function in the three-body system can be expanded by the two-body energy eigenstates. In case of the $\bar{K}N$ subsystem, for which the lowest energy is -11 MeV for the quasibound $\bar{K}N$ state, $\mathcal{E}_{\bar{K}N} \geqslant -11$ MeV and $\mathcal{E}^{I_1=0}_{\bar{K}N} \geqslant -11$ MeV should be always satisfied.

We also introduce quantities characterizing the structure of the three-body system, such as spatial configurations of the constituent particles and probabilities to have specific isospin configurations. These values are calculated as expectation values of the wave functions.

The root-mean-square (rms) radius of the $K\bar{K}N$ state is defined as the average of the distribution of K, $\bar{K}$, and N by

$$r_{K\bar{K}N} = \sqrt{\langle\Psi|\tfrac{1}{3}\left(\mathbf{x}_K^2 + \mathbf{x}_{\bar{K}}^2 + \mathbf{x}_N^2\right)|\Psi\rangle}, \tag{20}$$

which is measured from the center-of-mass of the three-body system. The rms values of the relative distances between two particles are calculated by

$$d_{\bar{K}N} = \sqrt{\langle\Psi|\mathbf{r}_1^2|\Psi\rangle}, \tag{21}$$

$$d_{KN} = \sqrt{\langle\Psi|\mathbf{r}_2^2|\Psi\rangle}, \tag{22}$$

$$d_{K\bar{K}} = \sqrt{\langle\Psi|\mathbf{r}_3^2|\Psi\rangle}. \tag{23}$$

Here r_1, r_2, and r_3 are the $\bar{K}N, KN$, and $K\bar{K}$ distances, respectively.

The probabilities for the three-body system to have the isospin $I_{K\bar{K}}$ states are introduced as

$$\Pi\left([K\bar{K}]_{I_{K\bar{K}}}\right) \equiv \langle\Psi|P_{\bar{K}}(I_{K\bar{K}})|\Psi\rangle, \tag{24}$$

where $P_{K\bar{K}}(I_{K\bar{K}})$ is the projection operator for the isospin configuration $[[K\bar{K}]_{I_{K\bar{K}}}N]_{I=1/2}$, as introduced before. We calculate the probabilities that the three-body system has the isospin configurations of $[[\bar{K}N]_{I_{\bar{K}N}}]_{I=1/2}$, where the total isospin $1/2$ is given by combination of total isospin $I_{\bar{K}N}$ for the $\bar{K}N$ subsystem and the kaon isospin $1/2$:

$$\Pi\left([\bar{K}N]_{I_{\bar{K}N}}\right) \equiv \langle\Psi|P_{\bar{K}N}(I_{\bar{K}N})|\Psi\rangle, \tag{25}$$

where $P_{\bar{K}N}(I_{\bar{K}N})$ is again the isospin projection operator.

III. RESULTS

In this section, we show the results of investigation of the $K\bar{K}N$ system with $I = 1/2$ and $J^P = 1/2^+$. We consider two parameter sets (A) and (B) for the two-body interactions listed in Table I. For the $\bar{K}N$ interactions, we use (A) the HW-HNJH potential and (B) the AY potential. For the $K\bar{K}$ and KN interactions, we use the phenomenological interactions derived in Sec. II B2 and II B3: KK(A) and KN(A) for set (A), and KK(B) and KN(B) for set (B). In addition, we study the effect of the KN repulsion by switching off the KN interaction in the parameter sets (A) and (B).

TABLE II. Energies of the $K\bar{K}N$ states calculated with the parameter sets (A) and (B) given in Table I. The results without the KN repulsive interaction are also shown. Contributions of $V^{I=0,1}_{\bar{K}N}$ and $V^{I=0,1}_{K\bar{K}}$ to the imaginary energy are separately listed. Partial energies, kinetic energies, and potential energies for two-body subsystems in the $K\bar{K}N$ state are also shown. Details of the definitions are explained in the text.

Parameter set	(A)	(A)	(B)	(B)
$V_{\bar{K}N}$	HW-HNJH	HW-HNJH	AY	AY
V_{KN}	On	Off	On	Off
ReE	-19	-39	-41	-57
$\langle T\rangle$	169	282	175	227
$\langle \mathrm{Re}V\rangle$	-188	-320	-216	-284
ImE	-44	-72	-49	-63
$\langle \mathrm{Im}V^{I=0}_{\bar{K}N}\rangle$	-17	-30	-19	-23
$\langle \mathrm{Im}V^{I=1}_{\bar{K}N}\rangle$	-1	0	0	0
$\langle \mathrm{Im}V^{I=0}_{K\bar{K}}\rangle$	-1	-10	-4	-10
$\langle \mathrm{Im}V^{I=1}_{K\bar{K}}\rangle$	-25	-31	-25	-31
$\langle T_{\bar{K}N}\rangle$	113	185	131	157
$\langle \mathrm{Re}V^{I=0}_{\bar{K}N}\rangle$	-87	-152	-139	-162
$\langle \mathrm{Re}V^{I=1}_{\bar{K}N}\rangle$	-2	0	0	0
Re$\mathcal{E}_{\bar{K}N}$	25	33	-9	-4
Re$\mathcal{E}^{I_1=0}_{\bar{K}N}$	-6	-4	-28	-27
$\langle T_{K\bar{K}}\rangle$	104	162	86	115
$\langle \mathrm{Re}V^{I=0}_{K\bar{K}}\rangle$	-4	-42	-11	-31
$\langle \mathrm{Re}V^{I=1}_{K\bar{K}}\rangle$	-101	-127	-75	-92
Re$\mathcal{E}_{K\bar{K}}$	-1	-7	-1	-7
$\langle T_{KN}\rangle$	59	108	55	83
$\langle \mathrm{Re}V^{I=0}_{KN}\rangle$	0	0	0	0
$\langle \mathrm{Re}V^{I=1}_{KN}\rangle$	6	0	10	0
Re$\mathcal{E}_{KN}$	65	108	65	83

A. Properties of $K\bar{K}N$ state

First, we find that, in both calculations (A) with the HW-HNJH and (B) with the AY potentials, the $K\bar{K}N$ bound state is obtained below all threshold energies of the $\{\bar{K}N\}_{I=0} + K$, $\{K\bar{K}\}_{I=0} + N$ and $\{K\bar{K}\}_{I=1} + N$ channels, which correspond to the $\Lambda(1405) + K$, $f_0(980) + N$, and $a_0(980) + N$ states, respectively.[1] This means that the obtained bound state is stable against breaking up to the subsystems. We show the level structure of the $K\bar{K}N$ system measured from the $K + \bar{K} + N$ threshold in Fig. 2. The values of the real and imaginary parts of the obtained energies are given in Table II. The imaginary part of the energy is equivalent to the half width of the quasibound state. The contribution of each decay mode

[1] In the present calculation, because the $K\bar{K}$ interaction is adjusted to reproduce the f_0 and a_0 scalar mesons having the same mass and width, it is independent of the total isospin of the $K\bar{K}$ subsystem and the thresholds of $f_0(980) + N$ and $a_0(980) + N$ are obtained as the same value.

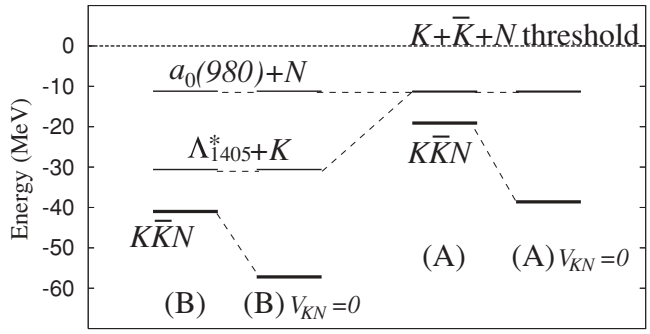

FIG. 2. Level structure of the $K\bar{K}N$ system calculated with (a) the HW-HNJH potential and (b) the AY potential. The energies are measured from the $K + \bar{K} + N$ threshold located at 1930 MeV. The $K\bar{K}N$ bound state is denoted by $K\bar{K}N$. The calculated thresholds of the two-body decays to $\{K\bar{K}\}_{I=0,1} + N$ and $\{\bar{K}N\}_{I=0} + K$ are denoted by $a_0(980) + N$ and $\Lambda^*_{1405} + K$, respectively. The results obtained without the KN repulsion are also shown.

to the imaginary energy is shown as an expectation value of the imaginary potential $\langle \mathrm{Im}V \rangle$ and the results obtained without the KN interaction are also given.

Let us discuss first the results with the KN interaction in detail. The binding energy of the $K\bar{K}N$ state measured from the three-body $K + \bar{K} + N$ threshold is larger in the result with (B) than that with (A), as found to be -19 MeV and -41 MeV in the cases of (A) and (B), respectively. This is because the AY potential gives a deeper binding of the $\{\bar{K}N\}_{I=0}$ state than the HW-HNJH potential due to the stronger $\bar{K}N$ attraction. These values have meaning just for the position of the quasibound state in spectrum. It is more physically important that the $K\bar{K}N$ bound state appears about 10 MeV below the lowest two-body threshold, $\{\bar{K}N\}_{I=0} + K$, in both cases (A) and (B). This energy is compatible to nuclear many-body system, and it is considered to be weak binding energy in the energy scale of hadron system. This weak binding system has the following significant feature. The width of the $K\bar{K}N$ state is estimated to be $\Gamma \sim 90$ MeV from the imaginary part of the energy. Comparing the results of the $K\bar{K}N$ with the properties of the two-body subsystems shown in Table I, it is found that the real and imaginary energy of the $K\bar{K}N$ state is almost given by the sum of those of $\Lambda(1405)$ and $a_0(980)$ [or $f_0(980)$], respectively. This indicates that two subsystems, $\bar{K}N$ and $K\bar{K}$, are as loosely bound in the three-body system as they are in two-body system.

The decay properties of the $K\bar{K}N$ state can be discussed by the components of the imaginary energy. As shown in Table II, among the total width $\Gamma = -2E^{\mathrm{Im}} \sim 90$ MeV, the imaginary potentials of the $\bar{K}N$ with $I = 0$ and the $K\bar{K}$ with $I = 1$ give large contributions as about 40 and 50 MeV, respectively. The former corresponds to the $\Lambda(1405)$ decay channel and gives the $\bar{K}N \to \pi\Sigma$ decay mode with $I = 0$. The latter is given by the $a_0(980)$ decay, which is dominated by $K\bar{K} \to \pi\eta$. In contrast, the $\bar{K}N$ $(I = 1)$ and the $K\bar{K}$ $(I = 0)$ interactions provide only small contributions to the imaginary energy. This is because, as we will see later, the $\bar{K}N$ subsystem is dominated by the $I = 0$ component due to the strong $\bar{K}N$ attraction and the $K\bar{K}$ subsystem largely consists of the $I = 1$ component as a result of the three-body dynamics. The small contributions of the $\bar{K}N$ $(I = 1)$ and the $K\bar{K}$ $(I = 0)$ interactions to the imaginary energy implies that the decays to $\pi\Lambda K$ and $\pi\pi N$ are suppressed. Therefore, we conclude that the dominant decay modes of the $K\bar{K}N$ state are $\pi\Sigma K$ and $\pi\eta N$. This is one of the important characters of the $K\bar{K}N$ bound system.

Although the obtained $K\bar{K}N$ state is located below the thresholds of $\Lambda(1405) + K$, $f_0(980) + N$, and $a_0(980) + N$, there could be a chance to access the $K\bar{K}N$ state energetically by observing the $\Lambda(1405) + K$, $f_0(980) + N$, and $a_0(980) + N$ channels in the final states, because these resonances have as large widths as the $K\bar{K}N$ state. Because, as we will show later, the $K\bar{K}N$ state has the large $\Lambda(1405) + K$ component, the $K\bar{K}N$ state could be confirmed in its decay to $\Lambda(1405) + K$ by taking coincidence of the $\Lambda(1405)$ out of the invariant mass of $\pi\Sigma$ and the three-body invariant mass of the $\pi\Sigma K$ decay.

Here we comment on theoretical uncertainty of the energy of the $K\bar{K}N$ state. In the present calculations, the $K\bar{K}$ interactions are obtained under the assumption that the $K\bar{K}$ attractive potentials provide $f_0(980)$ and $a_0(980)$ as quasibound states and are phenomenologically adjusted to reproduce the masses and the widths of $f_0(980)$ and $a_0(980)$. As discussed above, in the present result, the $K\bar{K}$ interaction with $I = 1$ gives the dominant contribution to the total width of the $K\bar{K}N$ state. We estimate theoretical uncertainty of the width of the $K\bar{K}N$ state by changing the inputs of the $a_0(980)$ width in the range from $\Gamma = 50$ to 100 as reported in PDG. We obtain the $\Gamma = 80 - 130$ MeV for the $K\bar{K}N$ state. We also find that the $K\bar{K}N$ state becomes unbound if the $K\bar{K}$ interaction with $I = 1$ is less attractive than 70% of the present values, in which $K\bar{K}$ with $I = 1$ is not bound in the two-body system.

We also show in Table II the values for the partial energies of the two-body subsystems, that is, decomposition of the kinetic and the potential energy in each subsystem. For the results (A) with the HW-HNJH potentials, the $\bar{K}N$ energy is found to be $\mathcal{E}_{\bar{K}N} = 25$ MeV, and the energy for the s-wave $\bar{K}N$ component, $\mathcal{E}^{l_1=0}_{\bar{K}N}$, is -6 MeV. The reason why $\mathcal{E}_{\bar{K}N}$ is much larger than $\mathcal{E}^{l_1=0}_{\bar{K}N}$ is that higher angular-momentum components in the $\bar{K}N$ subsystem, which provide large kinetic energy, mix into the dominant s-wave $\bar{K}N$ component because of the $K\bar{K}$ correlation in the $K\bar{K}N$ state. The energy $\mathcal{E}^{l_1=0}_{\bar{K}N} = -6$ MeV is not far from -11 MeV, which is used to fix the energy-dependent effective $K\bar{K}N$ interaction of the HW-HNJH potential, and the energy-dependence of the potential between these two values is so small that the results of the three-body system do not change.

Finally we discuss the role of the KN repulsion in the $K\bar{K}N$ system. In Fig. 2 and Table II, we show the results calculated without the KN interaction. We find that the binding energy of the $K\bar{K}N$ state is 20 MeV larger than the case of the calculation with the KN repulsion in both (A) and (B) cases and that the absolute value of the imaginary energy also becomes larger as $E^{\mathrm{Im}} = -72$ MeV and -63 MeV for (A) and (B), respectively. These values correspond to the $\Gamma = 130$–140 MeV width for the $K\bar{K}N$ state. The reason that the three-body system without the KN interaction has the more binding and the larger width is as follows. In general, the three-body system has less kinetic energy than the two-body system because of larger reduced

TABLE III. Isospin and spatial structure of the $K\bar{K}N$ state with the parameter sets (A) and (B) given in Table I. The results without the KN repulsive interaction are also shown. The r.m.s. radius of the K, $\bar{K}$, and N distribution, and the r.m.s. values for the $\bar{K}$-N, K-$\bar{K}$, and K-N distances are listed. The isospin components of the subsystems, $\bar{K}N$ and $K\bar{K}$ are also shown. The detailed definitions are described in Sec. IIC. The three-body wave function is obtained in the same way as that in Table II.

V_{KN}	(A) HW-HNJH On	(A) HW-HNJH Off	(B) AY On	(B) AY Off
	Isospin configuration			
$\Pi([\bar{K}N]_0)$	0.93	1.00	0.99	1.00
$\Pi([\bar{K}N]_1)$	0.07	0.00	0.01	0.00
$\Pi([K\bar{K}]_0)$	0.09	0.25	0.17	0.25
$\Pi([K\bar{K}]_1)$	0.91	0.75	0.83	0.75
	Spatial structure			
$r_{K\bar{K}N}$ (fm)	1.7	1.0	1.4	1.0
$d_{\bar{K}N}$ (fm)	2.1	1.3	1.3	1.2
$d_{K\bar{K}}$ (fm)	2.3	1.4	2.1	1.5
d_{KN} (fm)	2.8	1.6	2.3	1.6

mass in the three-body system. With less kinetic energy the system can localize more. As a result of the localization of the system, the system can gain more potential energy and larger imaginary energy in the case of no KN interaction than the case with the KN repulsion. In other words, thanks to the KN repulsion, the $K\bar{K}N$ state is weakly bound and its width is suppressed to be as small as the sum of the widths of the subsystems.

B. Structure of $K\bar{K}N$ state

We discuss the structure of the $K\bar{K}N$ system with $I = 1/2$. For this purpose, we analyze the wave functions obtained in the present few-body calculation in terms of the spatial structure and the isospin configuration of the $K\bar{K}N$ system.

We first investigate the isospin configuration of the $K\bar{K}N$ state. We show the isospin components of subsystems $\bar{K}N$ and $K\bar{K}$ in Table III. It is found that the $\bar{K}N$ subsystem has a dominant $I = 0$ component because of the strong $\bar{K}N$ interaction in the $I = 0$ channel. In the $K\bar{K}$ subsystem, the $I = 1$ configuration is dominant, whereas the $I = 0$ component gives minor contribution. This isospin configuration is caused by the following reason. In both $I = 0$ and $I = 1$ channels, the $K\bar{K}$ attraction is strong enough to provide quasibound $K\bar{K}$ states of $f_0(980)$ and $a_0(980)$. In addition, because these scalar mesons have similar masses and widths, the $K\bar{K}$ interactions in $I = 0$ and $I = 1$ adjusted to these masses and widths are similar to each other. In fact, we use the same parameters for the $K\bar{K}$ interactions in the present calculation, which gives isospin-blind potential. Therefore, the $\bar{K}N$ interaction plays a major role to determine the isospin configuration of the $K\bar{K}N$ state. Because the $\bar{K}N$ interaction has stronger attraction in the $I = 0$ channel than in the $I = 1$ channel, the system prefers to have $I = 0$ in the $\bar{K}N$ subsystem. If the $\bar{K}N$ subsystem has pure $I = 0$ configuration, which is the case without the KN repulsion, the $K\bar{K}$ subsystem should be composed by $I = 0$ and $I = 1$ with the ratio of 1:3 to have $I = 1/2$ of $K\bar{K}N$. Thus, the $\bar{K}N$ with $I = 0$ dominates the $K\bar{K}N$ system, and simultaneously the $K\bar{K}$ with $I = 1$ is dominant component. The small deviation from the pure $\bar{K}N(I = 0)$ configuration in the $K\bar{K}N$ state originates in the KN repulsion as indeed demonstrated in Table III.

Next we discuss the spatial structure of the $K\bar{K}N$ bound system. In Table III, we show the rms radius of $K\bar{K}N$, $r_{K\bar{K}N}$ defined in Eq. (20), and rms values for the $\bar{K}$-N, K-$\bar{K}$, and K-N distances, $d_{\bar{K}N}$, d_{KN}, $d_{K\bar{K}}$ defined in Eqs. (21), (22), and (23), respectively, in the $K\bar{K}N$ state. The rms distances of the two-body systems, $\{\bar{K}N\}_{I=0}$ and $\{K\bar{K}\}_{I=0,1}$, are shown in Table I. It is interesting that the present result shows that the rms $\bar{K}$-N and K-$\bar{K}$ distances in the three-body $K\bar{K}N$ state have values close to those in the quasibound two-body states, $\{\bar{K}N\}_{I=0}$ and $\{K\bar{K}\}_{I=0,1}$, respectively. This implies again that the two subsystems of the three-body state have very similar characters with those in the isolated two-particle systems.

The rms K-N distance is relatively larger than the rms $\bar{K}$-N and K-$\bar{K}$ distances due to the KN repulsion. The effect of the repulsive KN interaction is important in the present system. Without the repulsion, we obtain smaller three-body systems as shown in Table III. Especially the distances of the two-body subsystems are as small as about 1.5 fm, which is comparable with the sum of the charge radii of proton (0.8 fm) and K^+ (0.6 fm). For such a small system, three-body interactions and transitions to two particles could be important. In addition, the present picture that the system is described in nonrelativistic three particles might be broken down, and one would need relativistic treatments and two-body potentials with consideration of internal structures of the constituent hadrons.

Combining the discussions of the isospin and spatial structure of the $K\bar{K}N$ system, we conclude that the structure of the $K\bar{K}N$ state can be understood simultaneous coexistence of $\Lambda(1405)$ and $a_0(980)$ clusters as shown in Fig. 3. This does not mean that the $K\bar{K}N$ system is described as superposition of the $\Lambda(1405) + K$ and $a_0(980) + N$ states, because these states are not orthogonal to each other. The probabilities for the $K\bar{K}N$ system to have these states are 90% as seen in Table III. It means that $\bar{K}$ is shared by both $\Lambda(1405)$ and a_0 at the same time.

It is interesting to compare the obtained $K\bar{K}N$ state with nuclear systems. As shown in Table III, the hadron-hadron distances in the $K\bar{K}N$ state are about 2 fm, which is as large as nucleon-nucleon distances in nuclei. In particular, in the case (A) of the HW-HNJH potential, the hadron-hadron distances are larger than 2 fm and the rms radius of the three-body system

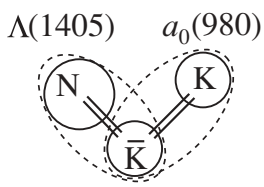

FIG. 3. Schematic structure of the $K\bar{K}N$ bound system.

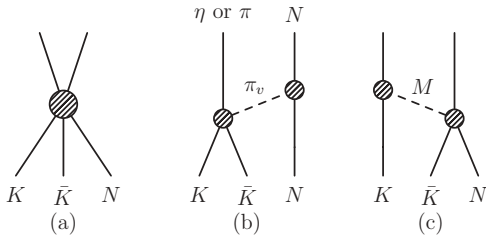

FIG. 4. Diagrams for the two-body decays. (a) Contact interaction. (b) Virtual pion exchange. (c) Virtual meson exchange. For (b) and (c), multimeson exchanges are also possible.

is also as large as 1.7 fm. This is larger than the rms radius 1.4 fm for ^{4}He. If we assume a uniform sphere density of the three-hadron system with the rms radius 1.7 fm, the mean hadron density is evaluated as 0.07 hadrons/(fm^3). Thus the $K\bar{K}N$ state has large spatial extent and dilute hadron density.

C. Possible two-body decay

The possible two-body decay modes of the three-body resonance are πN, ηN, $K\Lambda$, and $K\Sigma$. As described before, the present three-body system is spatially extended. In such systems with spatial extent and dilute hadron density, two-body decays are expected to be suppressed. Here we discuss the two-body decay widths under simple estimation based on geometrical argument. Let us first suppose that transitions of three-body bound state to two particles are induced by contact interactions as shown in Fig. 4(a). In such cases, the transition probability is proportional to square of density, $1/r^6$, where r is the radius of the three-body system, because the three particles should meet at a point for the contact interaction to take place. In the present calculation, the radius of the system is obtained as 1.7 fm in the parameter set (A). Thus, the two-body decay induced by the constant interaction is strongly suppressed by a factor $(0.8/1.7)^6 \sim 0.01$ in comparison with quark-model-like baryon resonances, if we assume their typical radius to be 0.8 fm.

Another possibility is two-body decay induced by two-particle transitions with virtual-meson exchanges as shown in Figs. 4(b) and 4(c). Decays without meson exchanges cannot occur due to energy conservation. The main contribution comes from virtual pion exchange for Fig. 4(b), because it has the longest interaction range. For Fig. 4(c), the pseudoscalar meson exchange is not possible, if the final states are restricted to two-body systems of the lowest-lying baryon and meson, because the three-point vertex of the pseudoscalar mesons break parity-invariance.[2] The two-particle transition probability is proportional to density, $1/r^3$, and thus, if the virtual pion exchange were infinite range, the suppression factor for the two-body decays induced by the meson exchange mechanism would be $(0.8/1.7)^3 \sim 0.1$ again in comparison with typical baryon resonances. In reality, the virtual pion can travel in finite distance. Thus, the two-body decays will be further strongly suppressed, because the hadron-hadron distances in the present three-body system are larger than the pion Compton length (1.4 fm). For quantitative evaluation of the decay width, further study is necessary.

It is also worth discussing that the small two-body decay induced by the virtual pion exchange have a selective decay pattern due to isospin symmetry. As shown in Table III, the $K\bar{K}$ subcomponent of the three-body system has dominantly the $I = 1$ configuration. Consequently, for the decay process in Fig. 4(b), the final state is selectively ηN thanks to the $K\bar{K} \to \pi_v\eta$ of the two-particle transition with $I = 1$. Therefore, the main two-body decay mode of the present three-body resonance is ηN.

IV. SUMMARY

We investigated the $K\bar{K}N$ system with $J^p = 1/2^+$ and $I = 1/2$ in nonrelativistic three-body calculation. We have used the effective $\bar{K}N$ potentials proposed by Hyodo-Weise and Akaishi-Yamazaki, which reproduce the $\Lambda(1405)$ as a quasibound state of $\bar{K}N$. The $K\bar{K}$ interactions are determined so as to reproduce $f_0(980)$ and $a_0(980)$ as quasibound states in $K\bar{K}$ with $I = 0$ and $I = 1$ channels, respectively. The potentials of KN are adjusted to provide the accepted KN scattering lengths, having strong repulsion in $I = 1$ and no interaction in $I = 0$. The present three-body calculation suggests that a weakly quasibound state can be formed below all threshold energies of the $\Lambda(1405) + K$, $f_0(980) + N$, and $a_0(980) + N$. The calculated energies of the quasibound state are -19 and -41 MeV from the $K\bar{K}N$ threshold in the results with HW and AY potentials, respectively. The width for three-hadron decays is estimated to be $90 \sim 100$ MeV. It has been found that the binding energy and the width of the $K\bar{K}N$ state is almost the sum of those in $\Lambda(1405)$ and $a_0(980)$.

Investigating the structure of the $K\bar{K}N$ system, we have found that, in the $K\bar{K}N$ state, the subsystems of $\bar{K}N$ and $K\bar{K}$ dominate the $I = 0$ and $I = 1$, respectively, and that these subsystems have very similar properties with those in the two-particle systems. This leads that the $K\bar{K}N$ quasibound system can be interpreted as coexistence state of $\Lambda(1405)$ and $a_0(980)$ clusters and $\bar{K}$ is a constituent of both $\Lambda(1405)$ and $a_0(980)$ at the same time. As a result of this feature, the dominant decay modes are $\pi\Sigma K$ from the $\Lambda(1405)$ decay and $\pi\eta N$ from the $a_0(980)$ decay, and the decays to $\pi\Lambda K$ and $\pi\pi N$ channels are suppressed. We have discussed smallness of the two-body decays based on geometrical argument. We have found that, among the small two-body decays, the dominant two-body decay mode is ηN.

We also have found that the rms radius of the $K\bar{K}N$ state is as large as 1.7 fm and the interhadron distances are lager than 2 fm. These values are comparable to, or even larger than, the radius of ^{4}He and typical nucleon-nucleon distances in nuclei, respectively. Therefore, the $K\bar{K}N$ system more spatially extends compared with typical hadronic systems. These features are caused by weakly binding of the three hadrons, for which the KN repulsive interaction plays an important role.

[2] $K^*\Lambda$ and $K^*\Sigma$ in the final state would be possible with the virtual pion exchange by $K\pi_v \to K^*$. But these are not two-body decays, because $K^*\Lambda(\Sigma)$ decays finally to $K\pi\Lambda(\Sigma)$.

The present calculation of the three-body wave function is based on the perturbative treatment of the imaginary potential. It is certainly necessary to study the details of the three-body resonance, especially the pole position, in more elaborated calculations, such as Faddeev type approach based on chiral effective theory. According to the discussion in the case of the two-body system, the pole position would be higher for the real energy than that of our result, whereas the imaginary energy would be similar. It is also interesting to investigate energy spectrum of this resonance in the real energy axis, which is directly accessible in experiments. Presence of the three-body N^* resonance at 1.9 GeV could affect spectrum of $\Lambda(1405)$ production, for instance, performed at SPring8 [28].

ACKNOWLEDGMENTS

The authors thank Professor Akaishi, Dr. Hyodo, Dr. Doté, Professor Nakano, and Professor J. K. Ahn for valuable discussions. They are also thankful to members of Yukawa Institute for Theoretical Physics (YITP) and Department of Physics in Kyoto University, especially for fruitful discussions. This work is supported in part by the Grant for Scientific Research (Nos. 18540263, 20028004 and 20540273) from Japan Society for the Promotion of Science (JSPS) and from the Ministry of Education, Culture, Sports, Science and Technology (MEXT) of Japan. A part of this work is done in the Yukawa International Project for Quark-Hadron Sciences (YIPQS). The computational calculations of the present work were done by using the supercomputer at YITP.

APPENDIX: QUASIBOUND TWO-BODY STATES IN COMPLEX POTENTIALS

In the present calculation, the energy and width of the quasibound states are calculated in the perturbative treatment of the imaginary potential. In this appendix, we discuss the correspondence of the energy and width calculated by the perturbative treatment to those obtained in the calculation dealing fully with the imaginary potential in the case of the two-body systems.

To implement the imaginary part of the effective potential fully, we solve the two-body Schrödinger equation in momentum space, for instance, in the method given in Ref. [29]. For the $\bar{K}N$ system with $I = 0$, we find the quasibound states at $-2 - 23i$ MeV for the HW-HNJH potential and $-28 - 20i$ MeV for the AY potential, where the real energy is measured from the $\bar{K}N$ threshold. The imaginary energies in both cases and the real energy for the AY potential agree with those obtained by the perturbative method, which are given in Table I, whereas the real energy obtained in the HW-HNJH potential is 9 MeV higher than the value of the perturbative calculation. This will be because higher-order perturbative corrections give positive energy shift.

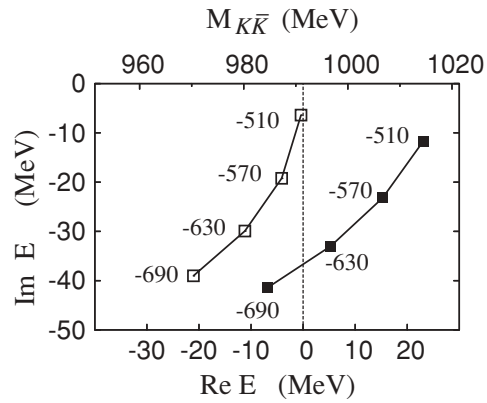

FIG. 5. The energy of the quasibound $K\bar{K}$ state calculated by perturbative (open squares) and nonperturbative (filled squares) treatments. The real part of the $K\bar{K}$ interaction is changed as $\mathrm{Re}U_{K\bar{K}} = -690, -630, -570, -510$ MeV. The imaginary part is fixed to be $\mathrm{Im}U_{K\bar{K}} = -210$ MeV. The range parameter is $b = 0.66$ fm [parameter set (B)]. The vertical dotted line denotes the $K\bar{K}$ threshold.

We also calculate the energy of the quasibound state of $K\bar{K}$ in the nonperturbative treatment of the imaginary potential. For the parameter set (B), we obtain $+5 - 33i$ MeV. [The case of the parameter set (A) is discussed in Sec. II B.] The real energy is measured again from the threshold of $K\bar{K}$. To obtain this solution, we selected the boundary condition for the state to be in the first Riemann sheet. This means that the $K\bar{K}$ channel is closed and the quasibound state is not a resonance decaying to $K\bar{K}$, although the state appears energetically above the $K\bar{K}$ threshold. It is interesting that the imaginary energy almost coincides again with the perturbative result.

To study the correspondence of the perturbative result and the nonperturbative calculation in which the quasibound state shows up above the threshold, we calculate the energies of the quasibound states by changing the strength of the real potential $\mathrm{Re}U_{K\bar{K}}$ from -690 MeV to -510 MeV. (The original strength is $U_{K\bar{K}} = -630 - 210i$ MeV.) In Fig. 5 we show the trajectories of the quasibound state energies both for the perturbative and nonperturbative treatments. This figure shows that the energies of the quasibound states smoothly vary as the depth of the real potential changes and also that the real energies between two treatments gets larger if the real energy of the perturbative calculation approaches the $K\bar{K}$ threshold. For the strengths $\mathrm{Re}U_{K\bar{K}} \geqslant -630$ MeV, we find that the nonperturbative real energies are 15–25 MeV higher than the perturbative results and they are numerically above the threshold, emphasizing that the imaginary energies are very similar in both calculations.

[1] R. H. Dalitz and S. F. Tuan, Phys. Rev. Lett. **2**, 425 (1959); Ann. Phys. **10**, 307 (1960).

[2] J. D. Weinstein and N. Isgur, Phys. Rev. Lett. **48**, 659 (1982); Phys. Rev. D **41**, 2236 (1990).

[3] P. Bicudo and G. M. Marques, Phys. Rev. D **69**, 011503(R) (2004).

[4] F. J. Llanes-Estrada, E. Oset, and V. Mateu, Phys. Rev. C **69**, 055203 (2004).

[5] T. Kishimoto and T. Sato, Prog. Theor. Phys. **116**, 241 (2006).
[6] A. Martinez Torres, K. P. Khemchandani, and E. Oset, Phys. Rev. C **77**, 042203(R) (2008).
[7] Y. Ikeda and T. Sato, talk in JPS meeting, September 2007, Hokkaido, Japan.
[8] Y. Kanada-En'yo and D. Jido, Phys. Rev. C **78**, 025212 (2008).
[9] Y. Akaishi and T. Yamazaki, Phys. Rev. C **65**, 044005 (2002).
[10] T. Yamazaki and Y. Akaishi, Phys. Lett. **B535**, 70 (2002).
[11] T. Yamazaki, A. Dote, and Y. Akaishi, Phys. Lett. **B587**, 167 (2004).
[12] T. Yamazaki and Y. Akaishi, Proc. Jpn Acad. B **83**, 144 (2007).
[13] N. V. Shevchenko, A. Gal, and J. Mares, Phys. Rev. Lett. **98**, 082301 (2007); N. V. Shevchenko, A. Gal, J. Mares, and J. Revai, Phys. Rev. C **76**, 044004 (2007).
[14] Y. Ikeda and T. Sato, Phys. Rev. C **76**, 035203 (2007).
[15] T. Yamazaki and Y. Akaishi, Phys. Rev. C **76**, 045201 (2007).
[16] A. Dote, T. Hyodo, and W. Weise, Nucl. Phys. **A804**, 197 (2008); A. Dote, T. Hyodo, and W. Weise, arXiv:0806.4917 [nucl-th].
[17] T. Hyodo and W. Weise, Phys. Rev. C **77**, 035204 (2008).
[18] E. Hiyama , Y. Kino, and M. Kamimura, Prog. Part. Nucl. Phys. **51**, 223 (2003).
[19] T. Hyodo, S. I. Nam, D. Jido, and A. Hosaka, Phys. Rev. C **68**, 018201 (2003); Prog. Theor. Phys. **112**, 73 (2004).
[20] T. Hyodo, D. Jido, and A. Hosaka, Phys. Rev. C **78**, 025203 (2008)
[21] D. Jido, J. A. Oller, E. Oset, A. Ramos, and U. G. Meissner, Nucl. Phys. **A725**, 181 (2003).
[22] J. A. Oller and U. G. Meissner, Phys. Lett. B **B500**, 263 (2001).
[23] D. Jido, A. Hosaka, J. C. Nacher, E. Oset, and A. Ramos, Phys. Rev. C **66**, 025203 (2002).
[24] W. M. Yao *et al*. (Particle Data Group), J. Phys. G **33**, 1 (2006).
[25] J. A. Oller and E. Oset, Nucl. Phys. **A620**, 438 (1997).
[26] J. A. Oller and E. Oset, Nucl. Phys. **A652**, 407 (1999).
[27] C. B. Dover and G. E. Walker, Phys. Rep. **89**, 1 (1982); O. Dumbrajs *et al*., Nucl. Phys. **B216**, 277 (1983).
[28] M. Niiyama *et al*., Phys. Rev. C (in press).
[29] Y. R. Kwon and F. Tabakin, Phys. Rev. C **18**, 932 (1978); R. H. Landau, Phys. Rev. C **27**, 2191 (1983).